Physical Characteristics of Arctic Stratus Clouds

SI-CHEE TSAY AND KOLF JAYAWEERA[1]

Geophysical Institute, University of Alaska, Fairbanks, AK 99701

(Manuscript received 4 June 1983, in final form 9 January 1984)

ABSTRACT

Observations of the physical properties of Arctic stratus clouds (ASC) over the Beaufort Sea area were made by the NCAR Electra aircraft during June 1980. The cloud morphology and microstructure observed during these experiments are described here. Arctic stratus clouds were formed under various meteorological conditions, but not when the axis of the Beaufort Sea ridge was zonal and the airflow into the region was continental.

The mean drop diameter in clouds observed under all conditions remained near 10 μm, while the mean liquid water content (LWC) was characteristic of the air mass forming the clouds and essentially determined by the mean drop concentration. Clouds showed considerable horizontal homogeneity but significant vertical changes occurred within them. The vertical profiles of LWC show that the values generally increased with height, as a result of an increase in droplet size rather than concentration. The drop size distribution near the base was monomodal, characteristic of condensation on a nucleus spectrum, but changed to a bimodal distribution near the top of the cloud.

1. Introduction

During the summer season, low-level stratiform clouds are a prevalent feature in the central Arctic. Monthly-averaged low cloud cover amounts compiled by Huschke (1969) and Vowinckel and Orvig (1970) show a steep increase during April to a broad maximum of nearly 70% for the summer months of May through September. This is followed by a rapid decrease during October to the winter value of less than 20%. The increase is attributed almost entirely to Arctic stratus clouds (ASC).

These clouds occur in the boundary layer and within the lower atmosphere below about 2000 m. They are tenuous, with thicknesses of a few hundred meters and are frequently observed to be laminated or comprised of two or more separate, well-defined layers (Jayaweera and Ohtake, 1973; Herman, 1977). These cloud layers interact with short- and longwave radiation, and hence exert an important influence on the heat balance of the surface pack ice. The importance of ASC on the surface radiation balance has been recognized by many authors, for example, Vowinckel and Orvig (1964, 1970), Herman (1977, 1980), and Herman and Goody (1976).

The meteorological processess that lead to the formation of ASC may occur over a wide range of scales. These clouds may be boundary-layer phenomena related to large scale advection of warm and humid air into the Arctic Basin, or they may generate and support themselves by approximately balanced budgets of water and energy. In addition to these processes, the structure of ASC is further determined by the optical and thermal properties of liquid water drops and ice crystals. Further discussion of the occurrence and principal characteristics of these clouds is given by the Polar Group (1980).

To understand the processes that form ASC, and the physical behavior of these clouds which are related to the Arctic planetary boundary layer and to the energy balance of the Arctic Basin, several elements must be considered, including the radiative and microphysical properties of the boundary layer, and synoptic weather situations. Although recent studies by Herman (1977, 1980) provide some radiative measurements, very little is known about the microphysical properties of ASC. Whatever is known about this subject is confined to bulk or average values for whole cloud systems measured using crude instruments (e.g., Koptev and Voskresensky, 1962; Jayaweera and Ohtake 1973; Kumai, 1973).

In this paper we present the observed physical characteristics of these clouds and attempt to describe these characteristics in terms of the prevailing meteorological conditions. Characteristics we present here are the cloud geometry and thicknesses; temperature, dew point and calculated relative humidity profiles, within and outside the cloud layer; droplet concentrations; size distribution; and liquid water content (LWC) profiles for the clouds. The data presented here are the results of the analysis of one of the three aspects of a complete Arctic Stratus Cloud experiment conducted jointly in June 1980 over the Beaufort Sea by the Universities of Alaska at Fairbanks, Wisconsin at

[1] Also Department of Physics.

Madison, and North Carolina State at Raleigh. The experiment was conducted in response to the recommendation of the Polar Subprogramme of the Global Atmospheric Research Programme (GARP publication series 19).

2. Experimental program

a. Instrumentation

The research platform for the measurement program was the National Center for Atmospheric Research (NCAR) Electra aircraft. In addition to instruments for measuring thermodynamic properties of the atmosphere, the aircraft was equipped with instrumentation for measuring cloud microstructure, radiation fields, and cloud nuclei.

The cloud droplet size distribution was measured using a Forward Scattering Spectrometer Probe (FSSP) manufactured by Particle Measuring Systems, Inc. (PMS) of Boulder, Colorado. This instrument was set to operate in the drop diameter range 2–47 μm; it resolves drops into 15 equally-spaced classes, i.e., 3-μm bins. The aircraft was also equipped with an Optical Array Cloud and Precipitation Probe (OAP), which operated in the size range 20–320 μm and again resolved particles into 15 bins. ASC are not expected to have water drops larger than about 50 μm in diameter, hence the primary purpose of this instrument was to count any ice crystals that may be present if ASC are supercooled. The other instrument for cloud physics was a Johnson–Williams (J–W) liquid water content meter. The J–W has an unstable zero offset but can generally be used to obtain LWC in stratus clouds. However, in our flights the J–W malfunctioned many times, and for flights where the instrument was thought to be working well, the zero offset was significantly unstable. Also, previous experience with this instrument in the Electra in ASC experiments (Herman, 1977) showed that it was unable to resolve the small amounts of LWC found in ASC. Therefore, we depended entirely on the FSSP for the determination of size distribution, concentration, and the liquid water content of the clouds.

The FSSP is the most widely used instrument for cloud droplet size distribution measurements. The instrument used in the NCAR Electra is an improved version of its predecessor, the Axially Scattering Spectrometer Probe (ASSP) described by Knollenberg (1976). Major problems resulting from coincidence and edge effect errors (Dye and Breed, 1979) are less important in the newer FSSP due to refinements in its optical and electronics systems (Knollenberg, 1981).

This version of the FSSP is the most reliable instrument available at present for the determination of size distribution and concentration of cloud droplets, especially those in stratus clouds. Dye and Baumgardner (1982) concluded that the concentrations measured by six FSSPs in their laboratory evaluations showed very good agreement at low concentrations. During the Cooperative Convective Precipitation Experiment (CCOPE), Breed and Dye (1982) found that an in-cloud comparison of droplet concentrations obtained by the FSSPs on six aircraft agreed to within 20%. This is a reasonable factor considering the variability inherent in the types of clouds in the sample. Laboratory tests using cloud guns, together with inflight tests and intercomparisons with identical properly aligned instruments, have shown consistent agreement in droplet size measurements to about 10% within the operating range of the instrument when droplet concentration is less than 4×10^8 m^{-3}. Since the LWC varies as a cube of the droplet radius, it could yield an error as high as 30% in LWC integrated from the concentration.

FSSP probes are not designed for the measurement of the LWC of clouds. However, the reliability of this instrument for the measurement of droplet concentration and LWC has been shown recently by several workers making comparisons with other instruments. For instance, Dye and Breed (1979) indicated that the shapes of LWC graphs integrated from the ASSP size distribution, whose shape would not be affected by coincidence error, had excellent agreement with the shape of the measured J–W. Telford and Wagner (1981) found that the FSSP deduced LWC and that measured by the J–W agreed to within a few percent. Also, Jiusto and Lala (1982) obtained very good comparisons of LWC between the FSSP and a carbon dioxide laser transmission (10.6 μm) system. Personne *et al.* (1982) made an extensive comparison between the FSSP, the J–W meter, and the Ruskin total water content probe, finding good agreement between LWC estimates among these probes after correcting for the undercounting by the FSSP when droplet concentration was very high ($\sim 7 \times 10^8$ m^{-3}).

Dye and Baumgardner (1982) pointed out that different FSSPs which are nominally configured the same, may perform differently. But, given the proper care, calibration, and processing of the data, and a consideration of the limitations of the instrument, an FSSP can provide reliable measurements. These precautions are routinely taken at NCAR.

The FSSP was checked, aligned, and calibrated by the manufacturer, prior to the field experiment and immediately after returning; the calibrations showed consistency. No calibration or alignment checks were made during the field season except for performance checks through housekeeping data packages. Data were recorded on magnetic tapes by the onboard data processing system. These data were later processed at NCAR.

Several investigators have discussed the applicability of the manufacturer's calibration in obtaining drop size and concentration. For example, Pinnick *et al.* (1981) found that the LWC obtained using the manufacturer's calibration differs by only 16% from the

modified Mie calibrations for atmospheric fog with drop radius less than 20 μm. Most of the differences occur in the drop radius range from 0.6 to 2 μm, and hence contribute very little error to the liquid water content. In conclusion, under constant air speeds and for concentrations less than 4×10^8 m^{-3}, FSSP data processed using the manufacturer's calibrations are applicable provided that regular checks are made to maintain proper alignment and clean optics.

b. *Measurements*

Data collection missions were flown for six days during June 1980. The flights originated from Eielson Air Force Base near Fairbanks, Alaska. The location of the experimental area is shown in Fig. 1. For the six days, a total of 22 hours of data was collected.

The selection of the days for experiments was determined by the location of suitable cloud decks, obtained from TIROS-N and NOAA-6 satellite imagery received at the National Weather Service office at Fairbanks.

The sampling runs started from above the stratus deck and descended through the cloud either to 100 m altitude if cloud base extended to below this height, or to 30 m above the sea-ice surface. Passes skimming the cloud tops and bases were also made to enable the reconstruction of the cloud geometry. The durations of the horizontal legs were 5–10 min.

3. Analysis: Computation of droplet size, concentration, and liquid water content

The computation procedures, provided by NCAR and based on the manufacturer's calibrations, are as follows.

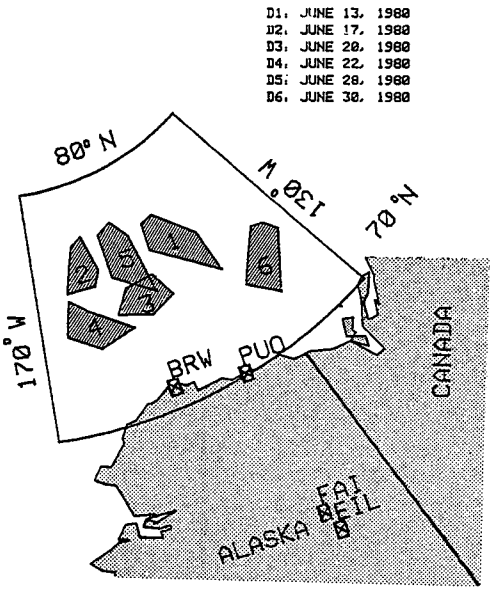

FIG. 1. Location map of experimental area.

The concentration of water droplets K_j in the jth channel of the FSSP is computed from the expression

$$K_j = C_j/(T_a S \Delta t),$$

where C_j is the count corrected for the dead time fraction in the jth channel during the time interval Δt, T_a is the true air speed, and S is the sampling area which is 4.17×10^{-7} m^2 for all FSSP channels. The average diameter for each channel is given by

$$D_j = j \times 3.13 \times 10^{-6} \text{ m}.$$

The total concentration of the drops, K, is obtained from summing over all the size channels, i.e.,

$$K = \sum_{j=1}^{15} K_j.$$

The liquid water content is therefore

$$W = \frac{\pi}{6} \rho \sum_{j=1}^{15} K_j D_j^3,$$

where ρ is the density of liquid water.

In presenting our results we will use the mean diameter D, and the diameter D_{95} below which 95% of the liquid water is contained, to represent the droplet spectrum. In the computation of D_{95} we determine the FSSP channel number, hence the mean diameter of the drops for that channel, below which the integrated LWC just exceeds 95% of the total. Therefore, the value of D_{95} is discrete and separated by 3.13 μm.

The values for LWC within a given cloud are compared with that obtained if an air parcel at the cloud base is lifted adiabatically through the cloud. The latter value is the maximum LWC the cloud could have at a given level and is referred to as adiabatic liquid water content.

4. Results

a. *Cloud morphology or geometry*

The macroscopic structure of the clouds is determined by reconstructing the cloud geometry as vertical cross sections. For convenience we have represented the cross sections in terms of longitudinal or latitudinal distance versus altitude (Figs. 2a and b). The stratiform characteristics of the ASC, together with the in-flight observations (visibility and existence of clouds below and above) and cloud boundaries determined from FSSP-measured drop concentration and derived LWC, were used to reconstruct cloud geometry. However, the movement of the entire system due to the prevailing wind was not taken into account. Each intercept point between airplane trajectory and cloud boundary is with respect to the ground. For instance, with respect to the ground the distances AD and BC in Fig. 2a are ~36 and 28 km, while the actual separation within the cloud should be about 60 and 50 km, respectively,

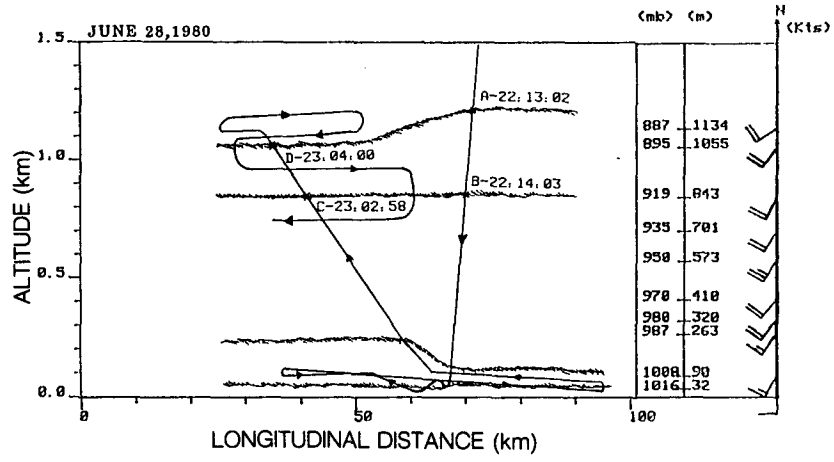

FIG. 2a. Reconstructed two-dimensional east–west cross section of clouds observed on 28 June.

which is AD or BC plus the component of the distance traveled by the system due to the prevailing wind of 10 m s^{-1} (~20 kt).

During the six days of experimentation, ASC were observed on five days, while on 17 June only altostratus was observed. Of the five days when ASC were observed, single-layer clouds were found on 13, 20, and 30 June, and multiple-layer clouds on 22 and 28 June.

b. Cloud microstructure

1) 13 JUNE 1980

Two distinct cloud bands, nearly 250-m thick and extensive in the north–south direction, were observed on this day. Their tops and bottoms were nearly uniform in height in this direction, but in the east–west direction such uniformity was observed only to the west. To the east, on the other hand, both the base and top of the clouds lifted by about 500 m within 100 km of longitudinal distance. This was the only occasion such a lifting was observed during the experiments.

Figure 3a shows a vertical profile for the cloud to the east. The initial position of penetration into the cloud layer was 73.9°N, 143.2°W. The basic situation was a northwesterly air flow colder than the sea-ice surface, and a cloud layer capped by an inversion layer with a 5°C temperature difference within a 450 m thickness. The atmospheric lapse rate under the cloud layer was conditionally unstable (Γ = 7.7°C km^{-1}), while within the cloud (Γ_c = 7.1°C km^{-1}) it was close to the saturated adiabatic lapse rate Γ_s = 7.2°C km^{-1}. The LWC generally increased with height but at a rate less than the adiabatic LWC; the droplet concentration was around 5×10^7 m^{-3} except near the cloud top; the diameter fluctuated around 12 μm and had a minimum value of 8 μm near the cloud base; and D_{95} was around 25 μm except at the upper and lower cloud boundaries, where it was around 38 μm. Therefore, bigger droplets existed near the cloud top and base.

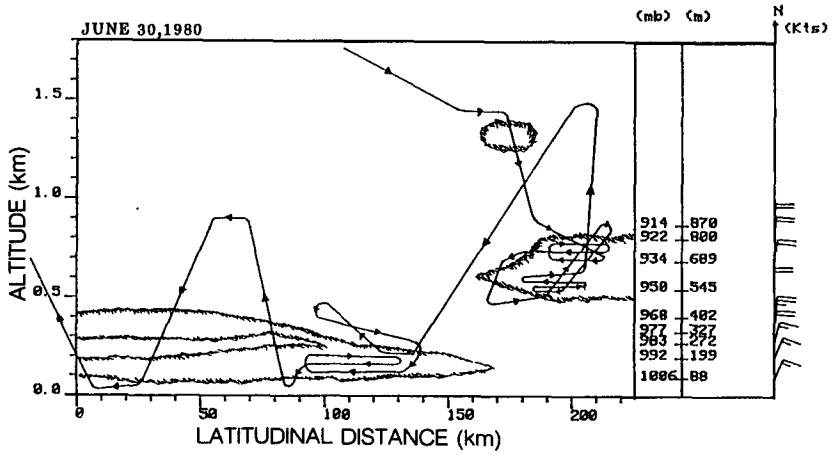

FIG. 2b. Reconstructed two-dimensional north–south cross section of clouds observed on 30 June.

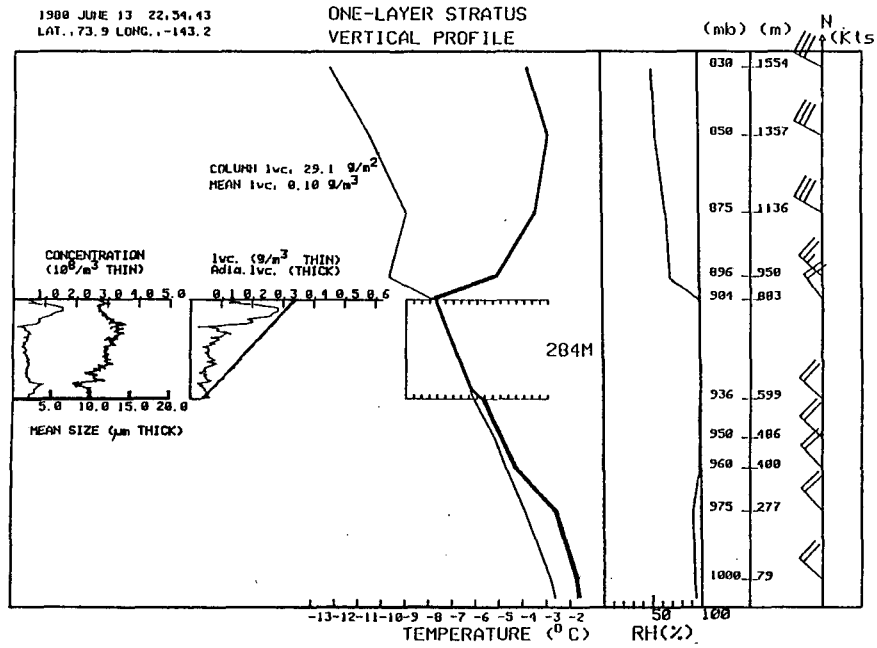

FIG. 3a. Vertical profile for the single-layer cloud on 13 June.

Figure 3b shows the horizontal leg of a 5-min run at the mean height of 860 m (20 m below cloud top); the first 2 min of data were observed closer to the cloud top. The correlation coefficient between concentration and LWC ws 0.86. However, there were substantial variations in concentration, which fluctuated with a frequency of roughly 1 min. The 95% diameter fluctuated within the range of 22–44 μm at approximately the same frequency, but the minimum value of the mean diameter was always within the range of the larger D_{95}. In other words, there were only a few larger droplets among the preponderance of smaller droplets.

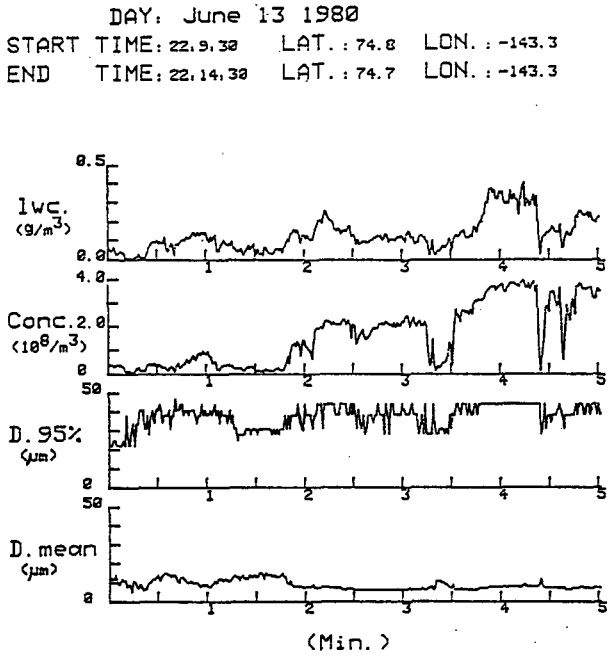

FIG. 3b. Horizontal leg for the cloud (280 m thick) observed on 13 June at 860 m height (20 m below cloud top).

A three-day sequence of 850-mb weather maps up to 13 June suggests that air in the experimental area had come from the Kara or Laptev Seas. The presence of a highly zonal ridge over the Beaufort Sea suggests that circulation from the south was blocked.

2) 20 JUNE 1980

The cloud observed on this day was a very low-level extensive sheet whose top, in general, was at a uniform height. The aircraft made no passes below 70 m due to lack of visibility, hence the location of the cloud base was not determined. The cloud top was well marked near 300 m.

Figure 4a shows the vertical profile for a descending run into a cloud layer at 73.7°N, 159.2°W. The basic feature was a southeasterly warm (above freezing) and dry air flow aloft. The cloud top was capped by a sharp inversion with a 9°C temperature difference within a 300 m thickness. The temperature lapse rate within the cloud layer was 8.2°C km^{-1}, which may have been caused by strong longwave radiative cooling from the cloud top. The droplet concentration was steadily maintained at around 2.5×10^8 m^{-3} (five times that measured on 13 June); the LWC increased with height and reached a maximum of 0.4 g m^{-3} near the cloud top. The correlation coefficient between droplet concentration and LWC was 0.63. The range of the mean diameter was from 8 to 12 μm, steadily increasing with

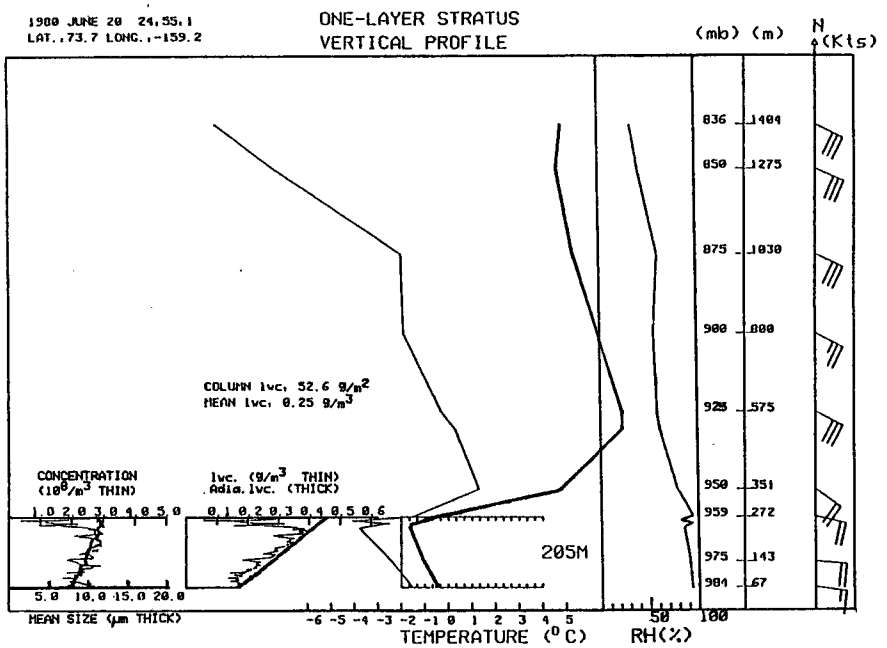

FIG. 4a. Vertical profile for the single-layer cloud on 20 June.

height; D_{95} was around 38 μm through the entire cloud layer.

Figures 4b and c show the horizontal legs of five-minute runs at the mean heights of 250 and 95 m, 50 and 200 m below the cloud top, respectively. It can be seen that the mean droplet diameter remained at 12 μm near the cloud top and 8 μm near the cloud base. The 95% diameters were around 38 μm at both locations, but had larger fluctuations near the cloud top. The values for the mean diameters and the 95% diameters at these heights agreed very well with the values obtained by the vertical profiling. This means

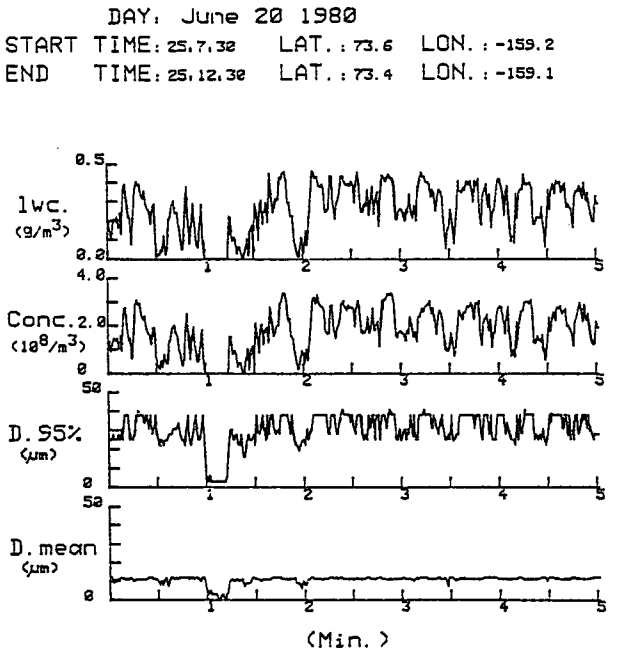

FIG. 4b. Horizontal leg for the cloud observed on 20 June at 250 m height (50 m below cloud top).

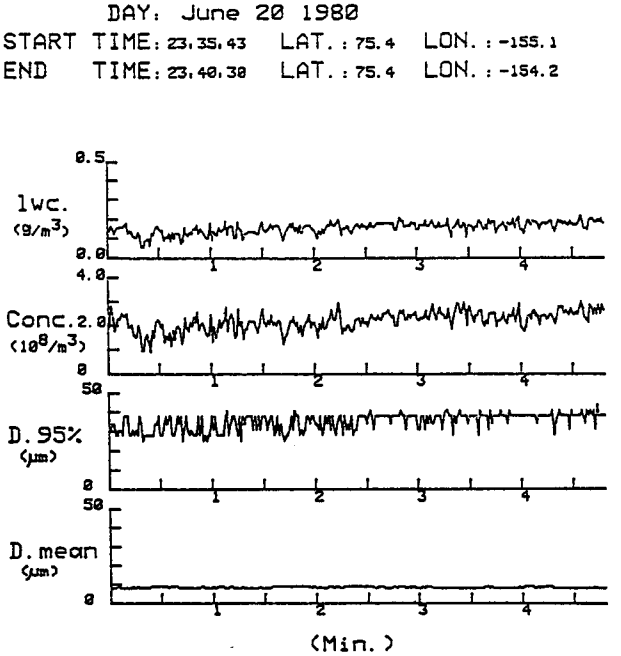

FIG. 4c. As in Fig. 4b, but for 95 m height (200 m below cloud top).

that the clouds had substantial horizontal uniformity in drop size distribution. The correlation coefficients between droplet concentration and LWC were 0.98 and 0.99 for near the cloud top and bottom, respectively. However, the concentration and LWC showed periodic variation at the cloud top, fluctuating approximately three times per minute.

A sequence of 850 mb weather maps suggests that the air mass at the experimental area originated in the interior of Alaska, traveled inside the state for two to three days, passed through the Brooks Range becoming a warm and dry continental air mass aloft, but may have undergone vertical motion at lower levels due to a Chukchi Sea low.

3) 22 JUNE 1980

Three well-defined layers, altostratus, an upper-layer ASC (430 m thick), and a lower-layer ASC (775 m thick) extending to nearly 100 m above the ice, were observed on this day. The lower cloud layers were fragmented. Sampling was done in the altostratus as well as in the various layers of stratus. Figure 5 shows the vertical profile made near 74.8°N, 165.6°W. The basic air flow was southwesterly at a temperature around 0°C.

The temperature and dew point profiles within these two cloud layers were very unusual. In the lower cloud, isothermal conditions were observed with an inversion just above the cloud top. A decrease in temperature occurred between the two layers and continued through the upper cloud and beyond at the rate of 7.7°C km^{-1}. The most surprising observation is that in both layers the air was undersaturated with respect to water with relative humidity as low as 70% in the upper cloud.

The droplet concentrations and liquid water content in both layers were low. In the lower ASC, the concentration fluctuated around 7×10^7 m^{-3}. The mean diameter fluctuated around 11 μm except for a minimum value of 7 μm near the inversion base and a maximum of 14 μm near the inversion top; the 95% diameter showed the same trend. The LWC decreased with height until it reached a minimum value of 0.05 g m^{-3} near the inversion base; it then increased with height until it reached a maximum of 0.2 g m^{-3} near the inversion top. The correlation coefficient between concentration and LWC was 0.5.

In the upper ASC, concentration increased with height and reached a maximum 100 m from cloud top; it then decreased with height. The LWC fluctuated around 0.09 g m^{-3}. The mean diameter was about 8 μm, except for a maximum of 12 μm near the cloud base, but the 95% diameter remained steadily around 14 μm throughout the entire layer.

The cloud geometry and the 850 mb weather maps from 0000 GMT 21 June suggest that the clouds were formed by a well-developed frontal system. Although a horizontal crossing of the frontal zone was not made, a comparison of air temperatures shows that the temperature of the air mass to the east was 1–2°C lower than that to the west, and the air aloft was warmer. This is typical of a warm-front occlusion. An east Siberian low occluded over the Chukchi Sea on June 21 and decayed during the following two days.

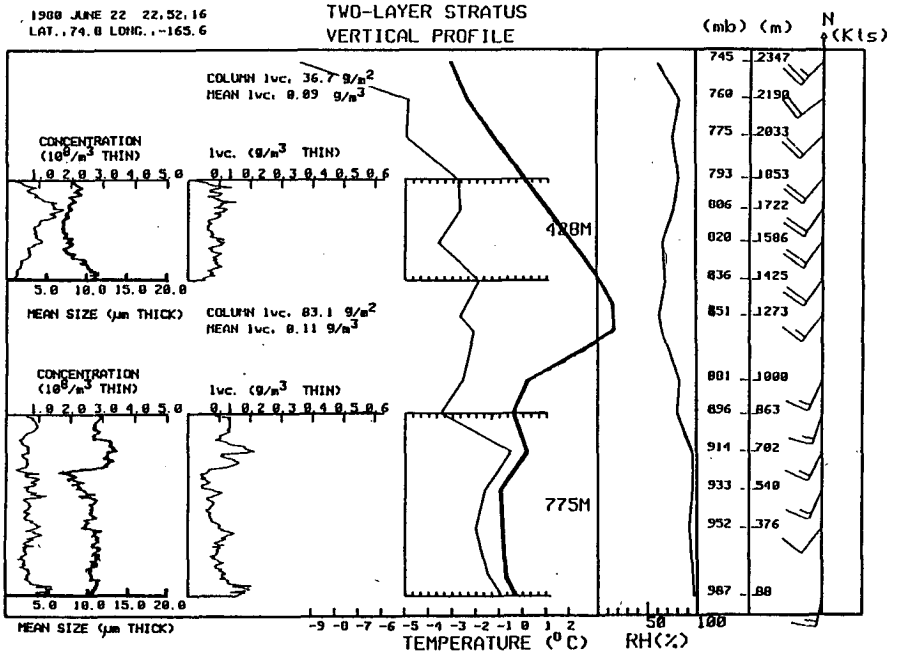

FIG. 5. Vertical profile for the multi-layer clouds on 22 June.

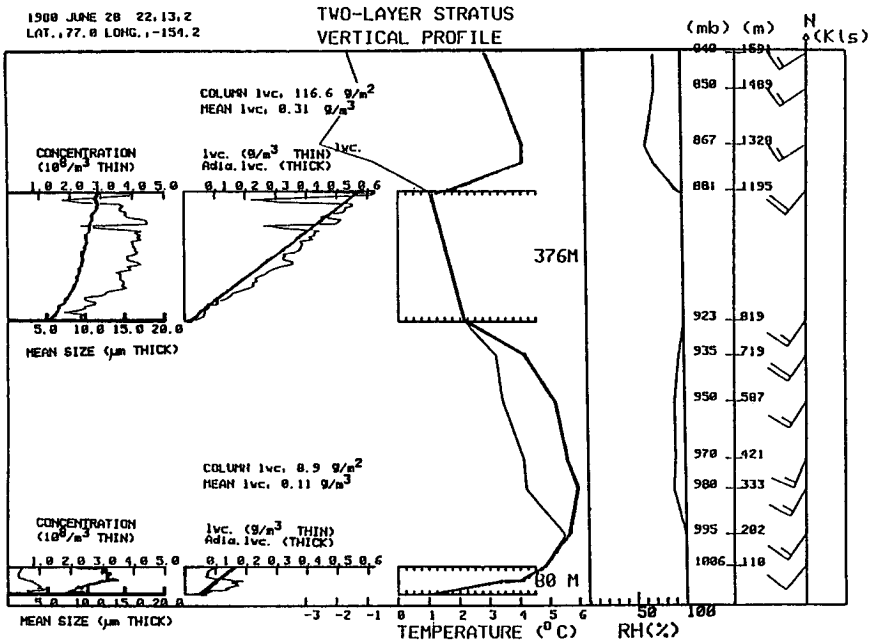

FIG. 6a. As in Fig. 5, but for 28 June.

4) 28 JUNE 1980

Two nearly parallel layers of stratus clouds were observed on this day (see Fig. 2a). The situation was similar to the observations of layering reported by Jayaweera and Ohtake (1973). The vertical profile observed during the descending run is shown in Fig. 6a. The temperature and humidity profiles indicate advection of warm humid air from the southwest at the levels where the clouds were observed. The upper cloud was capped by a strong inversion while inside the cloud the temperature profile was very close to saturated adiabatic (Γ_c = 5.7°C km^{-1}, while Γ_s = 6.0°C km^{-1}). The consistent overestimate of LWC exceeding the adiabatic value may be due to an incorrect assignment of cloud base resulting from sporadic precipitation. In the lower cloud, the temperature increased all the way from the bottom. The top of the inversion occurred at about the maximum height of the lower cloud, near 980 mb.

The upper cloud also showed some sporadic precipitation in the western section (Fig. 2a), which made determination of the cloud base difficult. However, inside this cloud on the horizontal leg at 940 m (110 m below cloud top as shown in Fig. 2a) the mean diameter was steady near 10 μm, but the droplet concentration showed considerable fluctuations as shown in Fig. 6b. The fluctuation of liquid water content followed that of droplet concentration, showing that LWC was controlled essentially by the concentration of drops.

The lower cloud showed similar consistency but with lower liquid water content and droplet concentrations. The correlation between LWC and concentration for both upper and lower clouds was near 0.83. Another interesting observation is that if the high-frequency fluctuations in concentration (or LWC) were smoothed out for the run shown in Fig. 6b, a wave form of period 2.5 min or ~16 km can be seen.

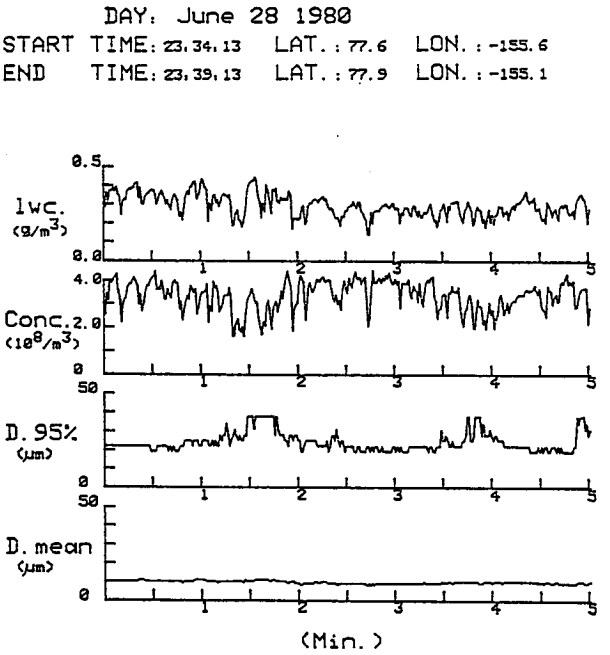

FIG. 6b. Horizontal leg for the cloud observed on 28 June at 940 m (110 m below cloud top).

A sequence of 850-mb weather maps from 0000 GMT 24 June suggests that the air mass at the experimental area had a continental origin in Siberia. However, it had sufficient time to gather moisture to form the upper cloud as it moved over the open Bering and Chukchi Seas. The lower cloud, on the other hand, may have formed by the mixing of the warm air with cold air over the pack ice.

5) 30 JUNE 1980

On this day we observed two single-layer cloud sheets; one in the north and the other in the south (see Fig. 2b). The microstructures of these two clouds however were quite different. The northern cloud was absolutely stable ($\Gamma_c = 5.2°C\ km^{-1}$, $\Gamma_s = 6.2°C\ km^{-1}$); LWC increased with height but was always less than the adiabatic LWC; the mean diameter increased linearly with height from 6 to 13 μm; the concentration fluctuated around $1.8 \times 10^8\ m^{-3}$ and D_{95} was $\sim 38\ \mu m$.

The southern ASC had two inversion layers; one was at the top of the cloud and the other, a very sharp inversion, was at the middle of this 314-m thick cloud. The LWC was less than the adiabatic LWC, the peak of the LWC and the mean droplet diameter were found at the beginning of the inversion layer, and D_{95} fluctuated around 30 μm. The concentration decreased with height from 1.5×10^8 to $8.0 \times 10^7\ m^{-3}$ (Fig. 7).

The weather situation at 1200 GMT 30 June suggests that the conditions had been essentially stagnant since 28 June. Because of this stagnant situation, and the similar microphysics such as mean droplet diameter and LWC observed for the upper cloud of 28 June and northern cloud of 30 June, we speculate that these two clouds were the same. Furthermore, satellite imagery showed continuous cloudiness over the area during this period.

If this contention is correct, then subsidence is an important mechanism for cloud dissipation which can have a greater effect than the tendency for an increase in cloud height due to longwave cooling. The top of the upper cloud of 28 June descended by 330 m over 46 hours ($2 \times 10^{-3}\ m\ sec^{-1}$). This gives a minimum estimate for the amount of subsidence, which is still much higher than the value of $10^{-4}\ m\ sec^{-1}$ assumed by Herman and Goody (1976). Similarly, the lower cloud layer may have been dissipated completely due to subsidence. For the lower-layer cloud, longwave cooling is not significant at the cloud top because of the presence of the upper cloud.

5. Discussion

We have presented observational data for ASC situations where single-layer clouds were observed on three days, multilayer clouds on two days, and an altostratus layer with no lower clouds on one day. Considerations of the cloud morphology, microstructure, and the meteorological situations allow us to gain insight into some aspects of ASC that are not yet well understood. These are:

1) What are the meteorological conditions conducive to the formation of ASC?

2) How are the cloud characteristics determined by the synoptic situation under which they are formed?

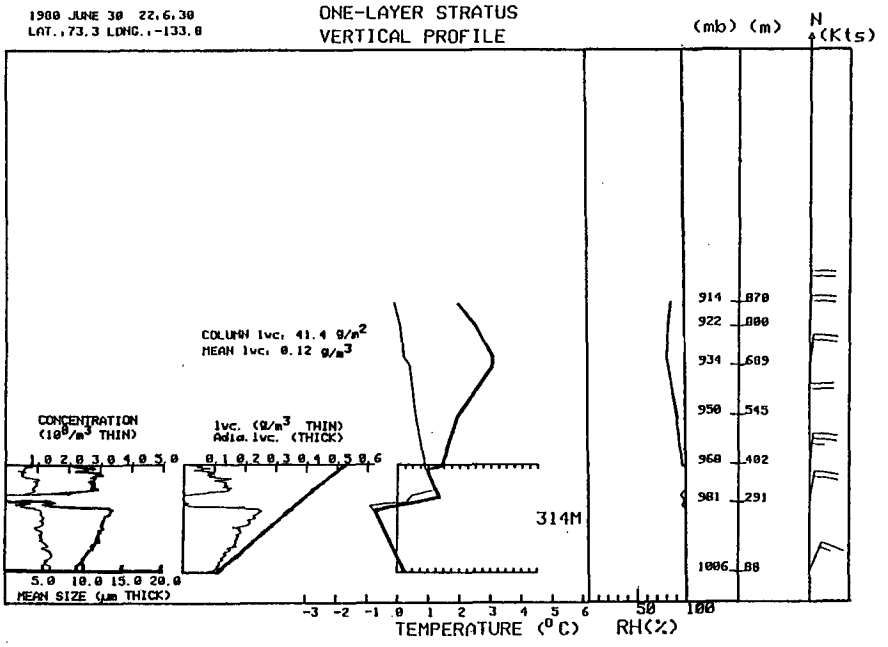

FIG. 7. Vertical profile for the southern cloud on 30 June.

3) What are the important processes that modify cloud structures after they are formed?

4) Could the LWC and drop size distribution profiles be expressed in terms of few parameters for incorporation into climatic models?

Although we do not anticipate conclusive answers to these questions, the inferences made from the observational data presented here will provide a useful basis for future research.

a. Meteorological conditions and cloud characteristics

By compiling meteorological situations in the summertime Arctic Basin, it is found that the Beaufort Sea high pressure system plays an important role. Occasionally, low pressure systems from the Bering or Chukchi Seas can also be found in this region. The ASC are observed in one of three synoptic situations: 1) the axis of the Beaufort Sea ridge is highly zonal (Fig. 8), driving cold air into the region (e.g., 13 June); 2) either the axis of the Beaufort Sea ridge is highly meridional (Fig. 9) or a low pressure system exists which drives warm air into the region (e.g., 28 and 20 June, respectively); or 3) an occluded and surviving frontal system exists and has a complicated microstructure (e.g., 22 June).

The characteristics of ASC essentially depend upon the air mass. Herman and Goody (1976) suggested that ASC may be formed when the atmosphere is either in a convective state or in a nonconvective state, depending on whether the air mass is initially colder or warmer than the sea-ice surface. A striking feature of their model calculation is that the top of the cloud formed in the convective state undergoes continuous lifting. This was observed from the cloud geometry of 13 June. Clouds formed in these situations have a high base and near-saturated adiabatic conditions exist below. The existence of ASC when the ridge axis is zonal is critically determined by the presence of air which has traveled over melting sea ice for a long period. The lack of ASC on 17 June under meteorological conditions similar to the 13 June case, except that the air entering the experimental area originated over dry land, supports this hypothesis. We may surmise that clouds occurred further north beyond the area of investigation.

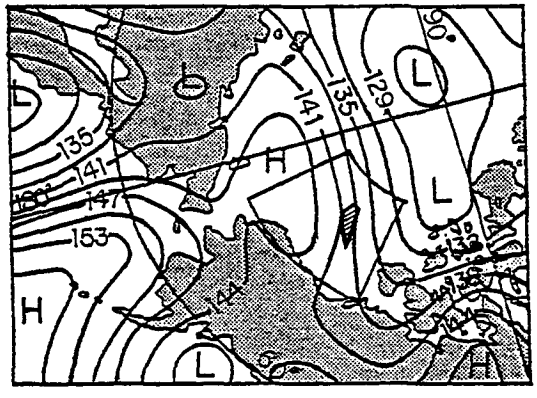

FIG. 8. 850 mb synoptic analysis for 0000 GMT 29 June 1980.

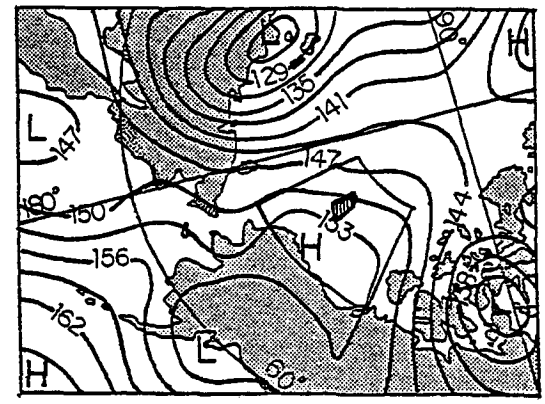

FIG. 9. 850 mb synoptic analysis for 0000 GMT 14 June 1980.

Clouds in nonconvective cases should then be formed by diffusive cooling of the air mass in contact with the sea ice. Once the clouds are formed radiative effects will influence their growth. On 20 June the lack of any clouds above may have caused the cloud top to cool giving rise to the observed strong inversion (6°C per 80 m) and a sufficient decrease in temperature above the cloud top to lift the cloud and lead to the observed near-adiabatic value in LWC (see Fig. 4a). We also observe that the vertical increase in LWC is due to an increase in size rather than concentration of the droplets. This observation is consistent with a cloud rising adiabatically and its droplets growing by condensation of the released moisture. On the other hand, the lower cloud of 28 June did not show the strong inversion due to radiative cooling because of the presence of the upper cloud, and it is clear from the temperature profile below 980 mb and the erratic LWC profile that its formation was due to mixing.

The upper cloud of 28 June was clearly due to the advection of warm moist air from the southwest. This air mass passed over considerable open water and entered the cold Arctic region without passing over any obstacles. The cloud formed as this air mass slowly ascended on the west side of the high pressure ridge.

Clouds formed under the nonconvective case are relatively thin and have very low bases which often reach the ice surface. Formation of any higher cloud layers is determined by the advection of moist air which undergoes ascending motion.

On two occasions our observations show LWC profiles close to adiabatic values. In this respect they are similar to those of Slingo *et al.* (1982) and Roach *et al.* (1982) for stratocumulus clouds observed over the North Sea during the Joint Air Sea Interaction Experiment (JASIN). Determinations by DeVault and Katsaros (1983) of total columnar liquid water content

from radiative flux measurements also show that LWC profiles may indeed follow adiabatic values. For the ASC and radiative cooling at cloud top or the gradual ascent of the air flow and inefficient mixing processes could explain the existence of adiabatic LWC values.

In summary, we find that ASC may be formed under very different meteorological situations. The large fractional cloud cover in the Arctic region may be explained because of the many conditions under which clouds are formed, but the morphology of any given cloud is very much dependent on the air flow.

b. *Cloud microstructure*

Cloud microstructure observations presented here show considerable similarities with those of stratus or stratocumulus clouds elsewhere, e.g., those reported by Telford and Wagner (1981) and Slingo *et al.* (1982). There is a marked horizontal homogeneity, except near the cloud top, in the average values of drop diameter, concentration, and LWC. Fluctuations in concentrations and LWC were observed only near the upper halves of cloud layers, while below this concentrations and LWC remained constant or increased with height. These fluctuations were wavelike, often separated by about 1 km. While the concentration changed by about a factor of 2, no significant change in mean size was observed. This suggests that dry air entrainment at the cloud top causes little change in the shape of the drop spectrum, but a substantial change in concentration. This observation is consistent with that reported by Slingo *et al.* (1982) and Telford and Wagner (1981).

The form of drop size distribution is important in the computation of radiative fluxes through the cloud (Tsay *et al.*, 1983) and provides information to assess the development of cloud microstructure. For all single cloud layers and for the upper cloud layers, the droplet distribution changed from a single mode near the cloud base to a double mode near the cloud top. An example of this for the upper layer cloud of 28 June is shown in Fig. 10. Bimodal distributions near cloud top have often been found in cumulus clouds (Warner, 1969). However, for these clouds the bimodal distribution is broader (peaks at 10 and 35 μm diameter) than for ASC (peaks at 6 and 16 μm diameter), suggesting that the drop size distribution is related to the nature of the clouds. Warner (1973) concluded that simple mixing between cloud and environment is unimportant in determining the drop size distribution.

Theoretical models of mixing processes have been proposed by many authors, for example, the homogeneous mixing model at Lee and Pruppacher (1977); the inhomogeneous mixing model of Latham and Reed (1977) and Baker *et al.* (1980); and the entity-type mixing of Telford and Wagner (1981) which is basically similar to the inhomogeneous mixing. All these models predict the evolution of a bimodal distribution in the regions where mixing takes places. Hallett (1983) indicated that the detail of the mixing process and its physical understanding are still unresolved problems.

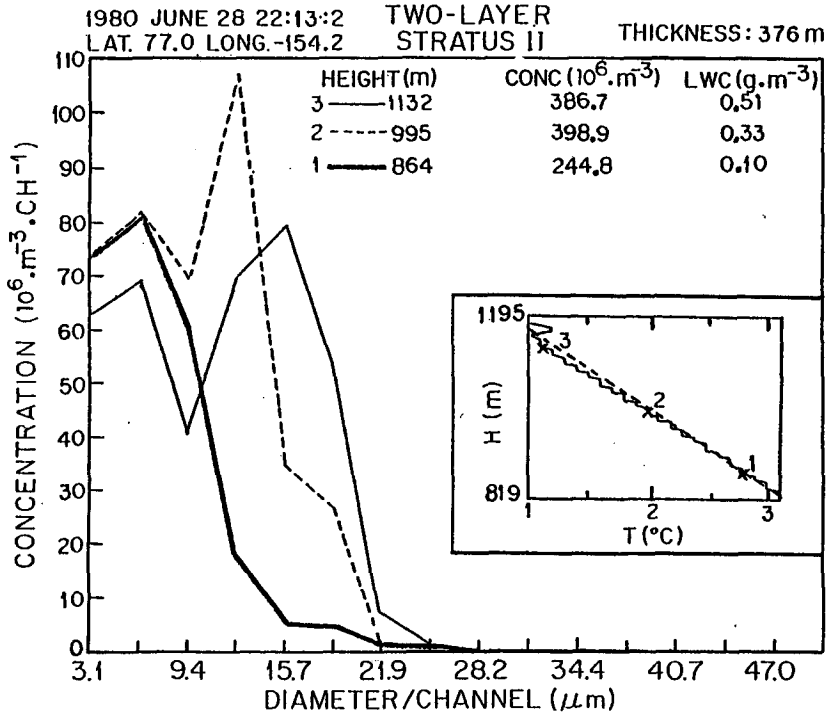

FIG. 10. Drop-size distribution measured at three different heights for the upper-layer cloud on 28 June.

TABLE 1. Average properties of Arctic stratus clouds observed during the six days of experimentation.

Date (June 1980)	Type	Flow	Base (m)	Thickness (m)	Concentration (10^6 m^{-3})	LWC (g m^{-3})	D (μm)	D_{95} (μm)
13	Single	NW	Variable	251	73 ± 52	0.09 ± 0.05	11.0 ± 3.0	28.9 ± 7.7
20	Single	SE	67*	233**	222 ± 72	0.21 ± 0.09	9.3 ± 1.2	34.8 ± 5.0
	Double:							
22	Top	SW	1425	428	76 ± 41	0.09 ± 0.05	9.8 ± 1.8	36.5 ± 6.3
	Bottom	SW	88	757	78 ± 40	0.10 ± 0.05	10.7 ± 1.8	30.0 ± 8.0
	Double:							
28	Top	SW	785	279	351 ± 104	0.27 ± 0.13	9.1 ± 1.6	23.2 ± 5.9
	Bottom	SW	53	115	81 ± 29	0.10 ± 0.04	10.3 ± 1.8	29.2 ± 6.2
	Single:							
30	North	N–NE	515	287	177 ± 30	0.17 ± 0.11	9.3 ± 2.0	34.9 ± 5.3
	South	N–NE	79	337	99 ± 33	0.11 ± 0.06	10.2 ± 2.4	24.2 ± 5.3
17	Altostratus	SW						
22		SW	3698	184	155 ± 62	0.06 ± 0.03	7.6 ± 1.0	17.9 ± 3.1
30		N–NE						

* Lowest aircraft altitude; cloud extended to sea-ice surface.
** Mean cloud top.

However, our observations show that in the upper half of the cloud where bimodal distributions are observed, the droplet concentration decreases vertically with height but fluctuates horizontally. Baker *et al.* (1980) predict that bimodal distributions occur through inhomogeneous mixing when the frequency of infiltration of the cloud by air parcels is low.

6. Conclusion

The average observed properties of ASC are given in Table 1. We find that ASC fall into two categories determined essentially by the type of air flow in which they form. If the clouds occur in cold polar air flowing over a warmer sea-ice surface, they are formed by a convective-type process. In the one case we observed, the cloud had an elevated base and a low LWC (13 June). On the other hand, if warm moist air flows over the Arctic Ocean, clouds form very near the sea-ice surface. In this situation more than one cloud layer may form depending on the availability of moisture aloft.

Arctic stratus clouds may also form as a result of occluded and surviving frontal systems. The microstructures of these clouds are different from the other two situations, and their morphologies are complex. The only situation not conducive to the formation of ASC occurs when the axis of the ridge is zonal and the air flow toward the Beaufort Sea is from the southeast or is in general of continental origin.

Qualitative considerations show that the predominant mechanism causing dissipation of ASC is large scale subsidence warming, especially when a lower layer is overlain by an upper layer, in which case longwave radiative cooling becomes less important for the lower layer.

Horizontal and vertical cloud microstructures suggest that inhomogeneous mixing of dry air occurs. However, the effect of entrainment is confined to the cloud top. The observed bimodal distribution of drop size in ASC can be predicted by the inhomogeneous mixing process when the frequency of infiltration of the cloud by air parcels is low.

A significant observation in ASC which are not formed by frontal passage is that the LWC profile in single-layer clouds or in the uppermost layer of multilayered clouds is nearly adiabatic near the cloud base. Large fluctuations, however, occur as the cloud top is reached. In general we suggest that a linear LWC profile following the adiabatic value, or a fraction thereof, may be used in computations of radiative effects of ASC.

Acknowledgments. This study was supported by the National Science Foundation through Grants DPP-77-20887 and DPP-81-11512. We thank the National Center for Atmospheric Research for providing the processed data tapes of the Electra research aircraft flights of June 1980. Special thanks go to Mr. Ted Fathauer and his staff of the National Weather Service, Fairbanks, for their kind assistance, and to Dr. G. Herman for coordinating the aircraft observational program and for many discussions on this subject.

REFERENCES

Baker, M. B., R. G. Corbin and J. Latham, 1980: The influence of entrainment on the evolution of cloud droplet spectra: I. A model of inhomogeneous mixing. *Quart. J. Roy. Meteor. Soc.*, **106**, 581–598.

Breed, D. W., and J. E. Dye, 1982: In-cloud intercomparisons of FSSP and J-W probes during CCOPE. *Preprints, Conf. on Cloud Physics*, Chicago, Amer. Meteor. Soc., 282–285.

DeVault, J. E., and K. B. Katsaros, 1983: Remote determination of cloud liquid water path from bandwidth limited shortwave measurements. *J. Atmos. Sci.*, **40,** 665–685.

Dye, J. E., and D. Baumgardner, 1982: Laboratory evaluations of six PMS FSSPs. *Preprints, Conf. on Cloud Physics,* Chicago, Amer. Meteor. Soc., 271–274.

——, and D. W. Breed, 1979: Microstructure of cloud in the high frequency hail area of Kenya. *J. Appl. Meteor.*, **18,** 95–99.

Hallett, J., 1983: Progress in cloud physics 1979–1982. *Rev. Geophys. Space Phys.*, **21,** 965–984.

Herman, G. F., 1977: Solar radiation in summertime Arctic stratus clouds. *J. Atmos. Sci.*, **34,** 1423–1432.

——, 1980: Thermal radiation in Arctic stratus clouds. *Quart. J. Roy. Meteor. Soc.*, **106,** 771–780.

——, and R. Goody, 1976: Formation and persistence of summertime Arctic stratus clouds. *J. Atmos. Sci.*, **33,** 1537–1553.

Huschke, R. E., 1969: Arctic cloud statistics from air calibrated surface weather observations. Mem. RM-6173-PR, Rand Corp., Santa Monica, CA, 79 pp.

Jayaweera, K., 1977: Characteristics of Arctic stratus clouds over the Beaufort Sea during AIDJEX. AIDJEX Bull., **37,** 135–152.

——, and T. Ohtake, 1973: Concentration of ice crystals in Arctic stratus clouds. *J. Rech. Atmos.*, **7,** 199–207.

Jiusto, J. E., and G. G. Lala, 1982: Liquid water content in radiation fogs. *Preprints, Conf. on Cloud Physics,* Chicago, Amer. Meteor. Soc., 300–302.

Knollenberg, R. G., 1976: Three new instruments for cloud physics measurements. *Proc. Int. Conf. on Cloud Physics,* Boulder, Amer. Meteor. Soc., 554–561.

——, 1981: Techniques for probing cloud microstructure. *Clouds, Their Formation, Optical Properties, and Effects,* P. V. Hobbs and A. Deepak, Eds., Academic Press, 15–91.

Koptev, A. P., and A. I. Voskresensky, 1962: On the radiation properties of clouds. *Proc. Arct. Antarct. Res. Inst. USSR,* **239,** 39–47. [Translation: Memo RM-5003-PR, Rand Corp., Santa Monica, CA, 1966.]

Kumai, M., 1973: Arctic ice fog droplet size distribution and its effects on light attenuation. *J. Atmos. Sci.*, **30,** 635–643.

Latham, J., and R. L. Reed, 1977: Laboratory studies of the effects of mixing on the evolution of cloud droplet spectra. *Quart. J. Roy Meteor. Soc.*, **103,** 297–306.

Lee, J. Y., and H. R. Pruppacher, 1977: A comparative study on the growth of cloud drops by condensation using an air parcel model with and without entrainment. *Pure Appl. Geophys.*, **115,** 523–545.

Personne, P., J. L. Brenguier, J. P. Pinty and Y. Pointin, 1982: Comparative study and calibration of liquid water content of clouds with small droplets. *J. Appl. Meteor.*, **21,** 189–196.

Pinnick, R. G., D. M. Garvey and L. D. Duncan, 1981: Calibration of Knollenberg FSSP light—scattering counters for measurement of cloud droplets. *J. Appl. Meteor.*, **20,** 1049–1057.

Polar Group, 1980: Polar atmosphere–ice–ocean processes: A review of polar problems in climate research. *Rev. Geophys. Space Phys.*, **18,** 525–543.

Roach, W. T., R. Brown, S. J. Caughey, B. A. Crease and A. Slingo, 1982: A field study of nocturnal stratocumulus I. Mean structure and budgets. *Quart. J. Roy. Meteor. Soc.*, **108,** 103–123.

Slingo, A., R. Brown and C. L. Wrench, 1982: A field study of nocturnal stratocumulus III. High resolution radiative and microphysical observations. *Quart. J. Roy. Meteor. Soc.*, **108,** 145–165.

Teleford, J. W., and S. Chai, 1980: A new aspect of condensation theory. *Pure Appl. Geophys.*, **118,** 720–742.

——, and P. B. Wagner, 1981: Observations of condensation growth determined by entity type mixing. *Pure Appl. Geophys.*, **119,** 934–965.

Tsay, S. C., K. Jayaweera and K. Stamnes, 1983: Dependence of radiative properties of Arctic stratus clouds on cloud microstructure. *Geophys. Res. Lett.*, **10,** 1188–1191.

Vowinckel, E., and S. Orvig, 1964: Energy balance of the Arctic. II. Longwave radiation and total radiation balance at the surface in the Arctic. *Arch. Meteor. Geophys. Bioklim.*, **B13,** 451–479.

——, and ——, 1970: The climate of the North Polar Basin. *World Survey of Climatology,* Vol. 14, *Climates of the Polar Regions,* S. Orvig, Ed., Elsevier, 129–252.

Warner, J., 1969: The microstructure of cumulus cloud. Part I. General features of the droplet spectrum. *J. Atmos. Sci.*, **26,** 1049–1059.

——, 1973: The microstructure of cumulus cloud. Part IV. The effect on the droplet spectrum of mixing between cloud and environment. *J. Atmos. Sci.*, **30,** 256–261.